Abdominal Aorta Blood Flow Analysis with Abaqus/CFD

Abaqus Technology Brief

Acknowledgement

Dassault Systèmes SIMULIA would like to thank Simpleware for providing the geometric model of the abdominal aorta.

Summary

The progression of disease in arteries is affected by local blood flow characteristics. Arterial structural features, such as branches, bifurcations, and irregular shape and curvature changes, introduce complexities to the blood flow field. Further insight on how such mechanical factors affect arterial health can be gained by employing computational fluid dynamics tools. With this approach, accurate and detailed quantitative data on hemodynamic factors can be obtained.

In this Technology Brief, we demonstrate the use of Abaqus/CFD to simulate complex blood flow in an abdominal aorta and its branches. Blood velocity profiles and wall shear stresses are computed, and flow recirculation is visualized. It will be shown that blood flow analyses using Abaqus/CFD can provide comprehensive data that would be difficult to obtain from experimentation.

Background

Many research studies have highlighted the importance of hemodynamic factors in vascular disease progression. The prevalence of disease in specific arterial locations is often correlated with flow features such as wall shear stress, stagnation, and recirculation zones.

For example, atherosclerotic lesions are more likely to be found along the outer wall of the carotid sinus region of the carotid artery where the wall shear stress is low, while they are less likely to occur along the inner wall of carotid sinus where the wall shear stress is high [1]. Similarly, atherosclerotic disease is more likely to develop in the abdominal aorta below the diaphragm [2]. Dilatation of the aortic wall in the abdomen as seen in aortic aneurysms is also affected by blood flow behavior; the growth and rupture of such aneurysms are affected by the hemodynamics [3]. Renal artery stenosis may also alter flow characteristics; narrowing of the artery can cause the blood flow regime to transition from primarily laminar to turbulent. Changes in the shear stress distribution affect the blood pressure as well as the evolution of atherosclerosis [4]. Surgical procedures such as coronary artery bypass, where grafts reroute blood flow across a blocked artery, can cause changes in flow characteristics that initiate a biological response such as local growth and remodeling of surrounding tissues.

In this Technology Brief, we show that Abaqus/CFD can be used to model the pulsatile blood flow in the abdominal aorta and its various branches that supply blood to the organs in the abdomen. Abaqus/CFD uses a time accurate transient incompressible viscous flow solver based on an advanced second-order projection method that uses a node-centered finite-element discretization for the pressure. This hybrid approach guarantees accurate solutions and preserves the local conservation properties associated with traditional finite volume methods. Abaqus/CFD can be used with unstructured grids and with various element types such as hexahedral, tetrahedral, wedge, and pyramid. The Abaqus/CFD solution methodology incorporates iterative Krylov solvers with algebraic multi-grid (AMG) preconditioning for solving the pressure-Poisson equation.

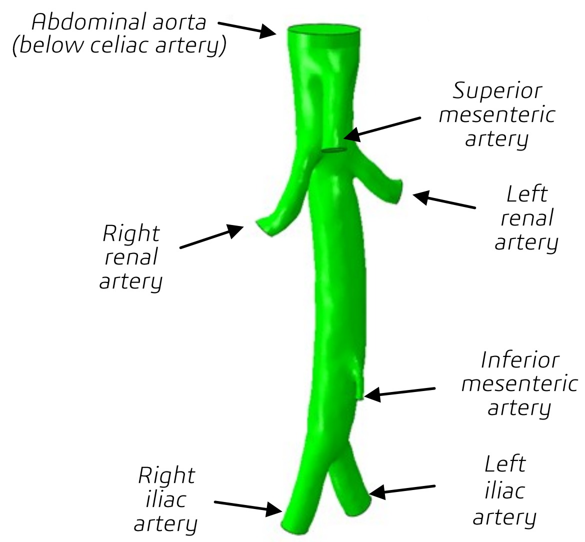

Figure 1: Abdominal aorta

Key Abaqus/CFD Features and Benefits

- Transient incompressible viscous fluid flow analysis
- Non-Newtonian viscosity models
- Luminal time dependent pressure waveform boundary conditions
- Pulsatile flow velocity boundary condition, derived from Womersley theory, implemented in a velocity user subroutine
- Third-party boundary layer mesh import in Abaqus/CAE

Geometry and Model

Patient-specific abdominal aorta geometry is obtained using the ScanIP software from Simpleware. ScanIP reads CT scan files and creates a high quality triangulation for STL export. The STL file of the abdominal aorta is imported into CATIA V6R2013. A surface reconstruction is performed to obtain the CAD model of the abdominal aorta. The geometry is then trimmed at the boundaries to make it suitable for CFD analysis. Figure 1 shows the final CAD model of the abdominal aorta and branches.

Mesh

The CAD model is imported into ANSA v13.1.4 and meshed with a boundary layer meshing technique. A total of 6 wedge layers are generated along the wall. The mesh consists of 192375 nodes and 568769 elements. Of these, 314873 are tetrahedral elements, 249660 are wedge elements and 4236 are hexahedral elements. The mesh is exported in the Abaqus input file format and then imported into Abaqus/CAE where the CFD analysis attributes are defined. A close-up view of the boundary layer mesh is shown in Figure 2.

Material

Blood is modeled as an incompressible fluid with a density ρ = 1050 kg/m^3 and a non-Newtonian viscosity described by the Carreau-Yasuda model. The model properties are listed in Table 1. The Carreau-Yasuda model describes the shear thinning behavior of blood. It is often a reasonable approximation to treat blood as a Newtonian fluid in blood vessels greater than 0.5 mm in diameter. In vessels of such large diameter, the viscosity is relatively constant due to high rates of shear. However, non-Newtonian effects need to be accounted for in smaller vessels. The dependence of viscosity on the shear rate, on a log-log scale, is shown in Figure 3.

Analysis Procedure

A transient incompressible laminar fluid flow analysis is performed in Abaqus/CFD. Abaqus/CFD uses a projection method that enables segregation of pressure and velocity fields for efficient solution of the incompressible Navier-Stokes equations. The advective and diffusive fluxes are both treated implicitly. The solution method uses a second-order accurate least-squares gradient estimation. Simulation is performed for 4 cardiac cycles, with each cycle lasting 0.9 sec.

Boundary Conditions

Solving the transient Navier-Stokes and continuity equations requires specification of appropriate initial and boundary conditions. Blood enters the abdominal aorta at a level below the celiac artery. The model has six outlet sections representing the major branches of the abdominal aorta: the superior mesenteric artery, the left and right renal arteries, the inferior mesenteric artery, and the left and right iliac arteries.

A no-slip/no-penetration wall boundary condition is applied on the wall surface of the abdominal aorta. A time-dependent luminal pressure waveform as shown in Figure 4 is applied at the left and right iliac artery outlets. The pressure waveform is a triphasic pulse appropriate for normal hemodynamic conditions in the abdominal aorta below the renal artery ([7], [8]). The volumetric flow rates

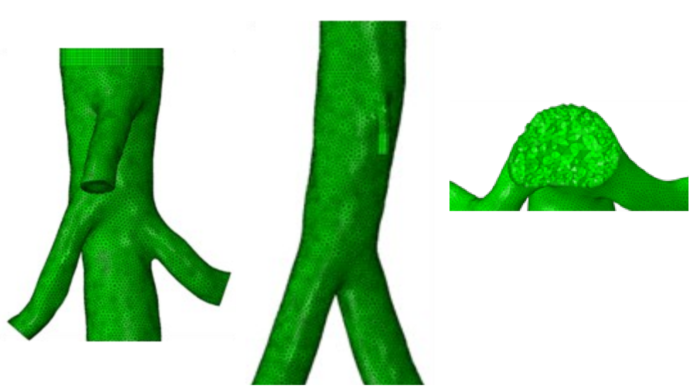

Figure 2: Boundary layer mesh of the abdominal aorta

Shear viscosity at low shear rates	0.025
Shear viscosity at high shear rates	0.0035
Time constant	25
Flow behavior index	0.25
Material constant	2.0

Table 1: Non-Newtonian fluid properties for the Carreau-Yasuda model

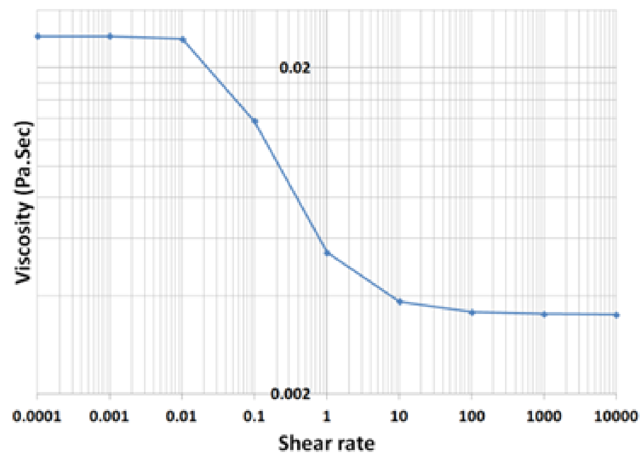

Figure 3: Viscosity v. shear rate for non-Newtonian blood properties

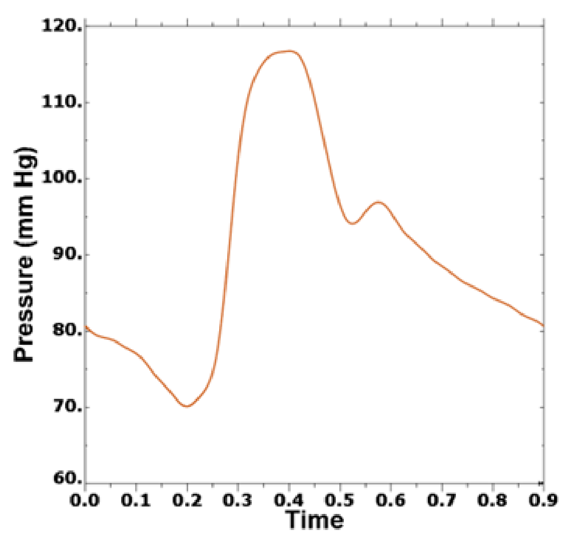

Figure 4: Luminal pulsatile pressure waveform

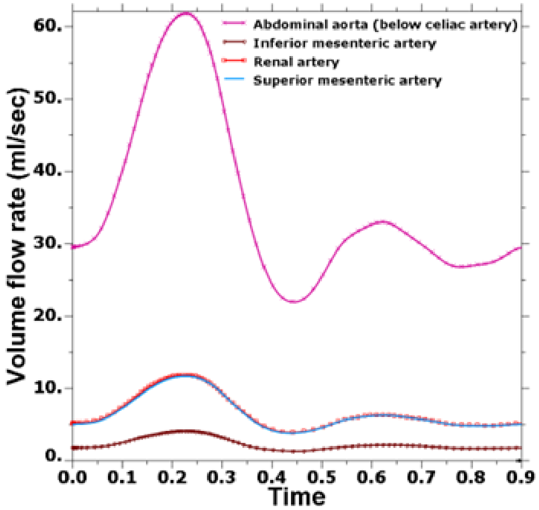

Figure 5: Flow rates for abdominal aorta, superior mesenteric artery, left and right renal artery, and inferior mesenteric artery

at the abdominal aorta inlet and superior mesenteric, left and right renal, and inferior mesenteric artery outlets are shown in Figure 5 ([5], [6]).

These flow rate waveforms are represented as complex Fourier series and their coefficients are utilized for evaluating the velocity boundary condition at the inlet and outlets (except for the left and right iliac artery):

$$Q(t) = Q_o + \sum_{k=1}^{N} \{ a_k \cos(k\omega t) + b_k \sin(k\omega t) \}$$

$$Q_o = \frac{1}{T}\int_0^T Q(t)dt, \quad a_k = \frac{2}{T}\int_0^T Q(t)\cos(k\omega t)dt$$

$$b_k = \frac{2}{T}\int_0^T Q(t)\sin(k\omega t)dt$$

$$Q_k = \begin{cases} \frac{1}{2}(a_k + ib_k) & k = -n,\ n < 0 \\ a_o & n = 0 \\ \frac{1}{2}(a_k - ib_k) & k = n,\ n > 0 \end{cases}$$

Here Q_k represents the complex Fourier coefficients of the flow waveforms. The velocity boundary condition is specified at the inlet and outlets through user subroutine `SMACfdUserVelocityBC`. The user subroutine calculates a spatially- and time-varying velocity boundary condition based on Womersley theory and the volume flow rates shown in Figure 5.

Womersley theory [9] evaluates the velocity profile at any cross-section for the unsteady, laminar flow of an incompressible fluid through a pipe of constant radius, when a time-varying pressure gradient is applied. The profile is defined as

$$u(r,t) = \frac{2Q_o}{\pi R^2}\left(1 - \frac{r^2}{R^2}\right) + \sum_{n=1}^{N} \mathrm{Real}\left\{ \frac{2Q_n}{\pi R^2} \left[\frac{1 - \dfrac{J_0\left(\alpha_n \frac{r}{R} i^{3/2}\right)}{J_0\left(\alpha_n i^{3/2}\right)}}{1 - \dfrac{2J_1\left(\alpha_n i^{3/2}\right)}{\alpha_n i^{3/2} J_0\left(\alpha_n i^{3/2}\right)}} \right] e^{in\omega t} \right\}$$

$$\alpha_n = R\sqrt{\frac{\rho n \omega}{\mu}}$$

In this equation, α_n is the non-dimensional Womersley number, where R denotes the radius, ρ the density, μ the viscosity and ω the circular frequency. Real(*) denotes the real part of a complex number and J_0 and J_1 are Bessel functions of the first kind of order 0 and 1, respectively.

The choice of the Womersley velocity profile is a significant improvement over spatially-constant or parabolic velocity profiles since it captures the flow reversal at artery outlets and provides a more realistic boundary condition for pulsatile flows. Womersley theory, however, is limited to circular cross-sections and hence, a mapping method ([10]) is used to map the evaluated velocity profile to non-circular cross-sections.

Velocity User Subroutine Implementation

User subroutine `SMACfdUserVelocityBC` is written in C and provides access to the necessary model and solution quantities. Access is also provided to the MPI communicator and MPI routines for parallel implementation. The following steps are performed in the user subroutine to calculate velocities on the inlet and outlets:

1. Find the facets of elements lying on the edge of the surface. This is accomplished using a convex hull algorithm for finding edge points amongst a point cloud.
2. Transform all surface points to a local coordinate system specified by the user and with its origin lying at the surface centroid.
3. Express the points in a polar coordinate system with its origin located at the surface centroid.
4. Evaluate a normalized radius [10]:
   - **a.** For each internal point (r, θ), find the two edge nodes *i* and *j* with θ coordinates such that $\theta_i \le \theta \le \theta_j$.
   - **b.** Evaluate a normalized radius R by linearly interpolating the radius of edge nodes, R_i and R_j. The normalized radius serves as the radius for all points lying on the line connecting an edge point to the centroid.
5. Evaluate the Womersley velocity using the radius r, normalized radius R, current time value, and Fourier coefficients for the flow waveform.
6. Transform the velocity to the global system for boundary condition specification.

The above procedure can be skipped for circular surfaces. For these cases, the radius of the circular surface serves as the normalized radius for all internal points.

Results and Discussion

The kinetic energy of the fluid domain is plotted in Figure 6. It can be seen that the analysis reaches a steady periodic condition after 1 cardiac cycle.

Figure 7 shows the velocity vectors along the midsagittal plane in the infrarenal segment of the abdominal aorta at various times during the cardiac cycle. A mildly recirculating flow pattern can be seen near the anterior wall; this vortex is formed during late systole and remains until peak systole when the effect of strong systolic acceleration results in a completely attached flow along the anterior wall. The particular location of the vortex is due to the curvature of the infrarenal segment which forces the flow to expand suddenly about the corner. The anterior portion of the abdominal aorta displays lower velocities than the core and posterior portion.

Wall shear stresses during the cardiac cycle are contoured in Figure 8. The shear stress magnitude can be used to estimate the possibility of rupture of aneurysms.

Figure 9 shows the surface traction vectors on the infrarenal segment of the abdominal aortic walls. Relatively low tractions are found compared to the branches where the velocities are higher. The primary movement of surface traction vectors is from the top of the vessel to the bottom, following the movement of the vortex during the cardiac cycle.

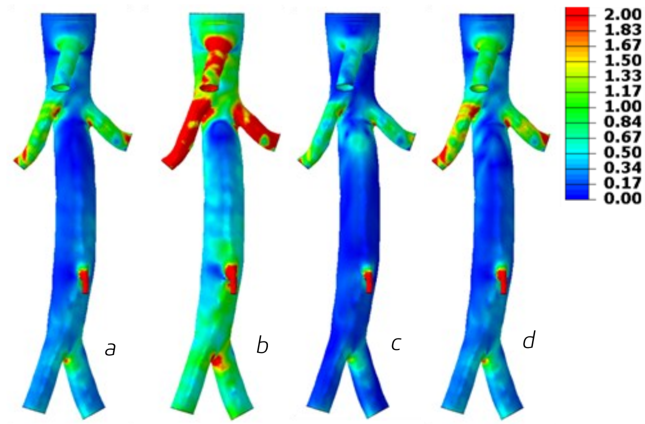

Figure 8: Wall shear stress (N/m²) at (a) the beginning of the cycle, (b) peak systole, (c) end systole, and (d) mid diastole

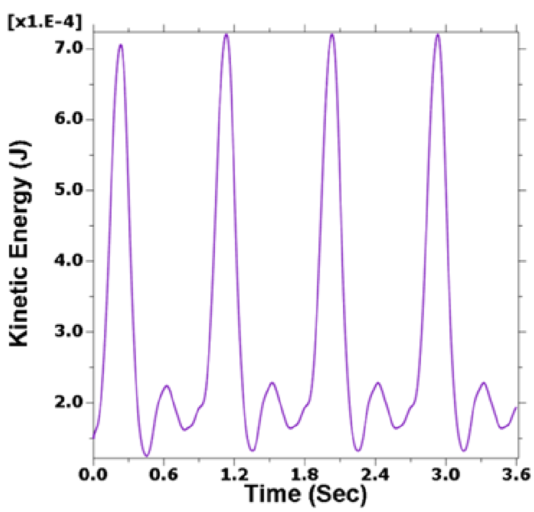

Figure 6: Total kinetic energy of the flow

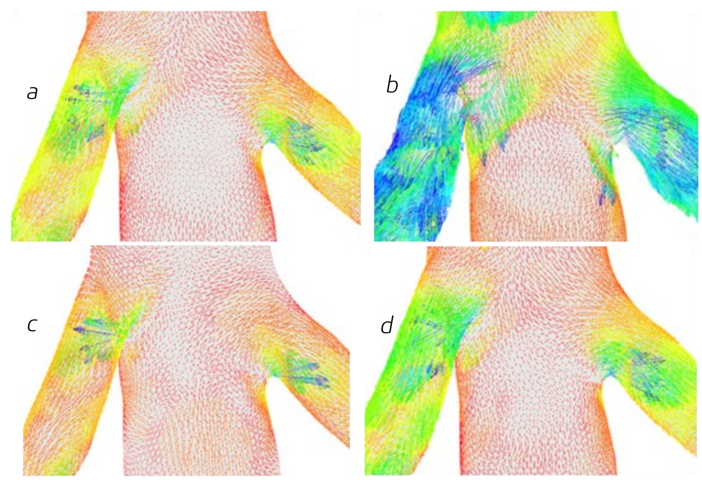

Figure 9: Surface traction (N/m²) vector plot in the infrarenal segment at (a) the beginning of the cycle, (b) peak systole, (c) end systole, and (d) mid diastole

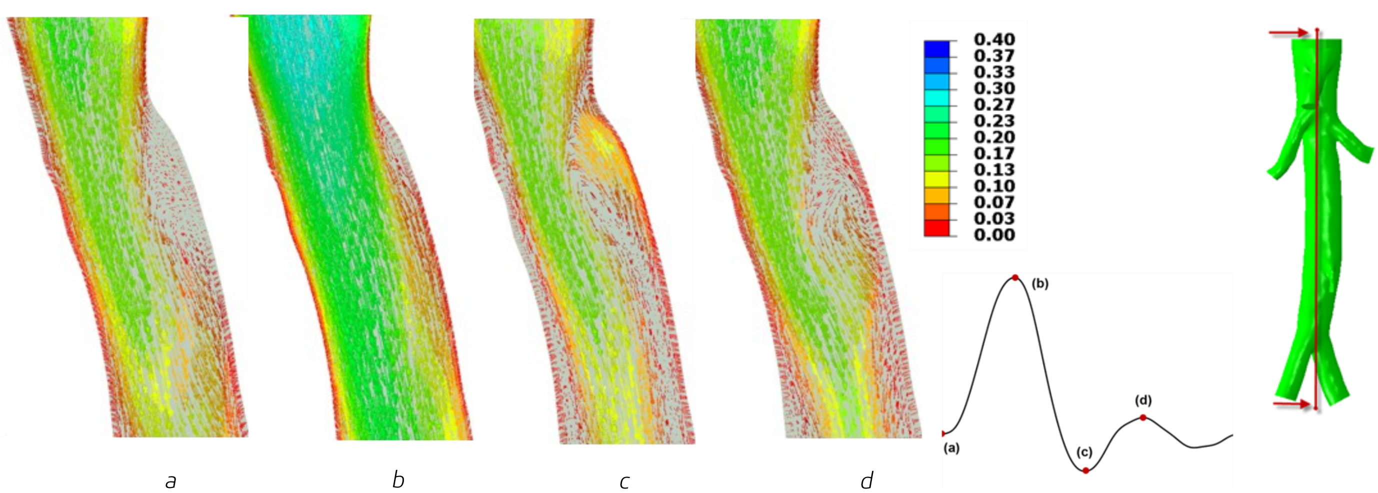

Figure 7: Velocity vector field (m/sec) along the midsagittal plane in the infrarenal segment of abdominal aorta at (a) the beginning of the cycle, (b) peak systole, (c) end systole, and (d) mid diastole. Midsagittal plane definition (far right) and schematic representation of various time points during cardiac pressure cycle

In Figure 10, streamlines are shown for the end systole. The streamlines show the formation of the vortex in the infrarenal segment and significant mixing of the blood. Figure 11 plots the percentage error in the mass balance, defined as the ratio of the sum of the inlet and outlet volume flow rates to the inlet volume flow rate.

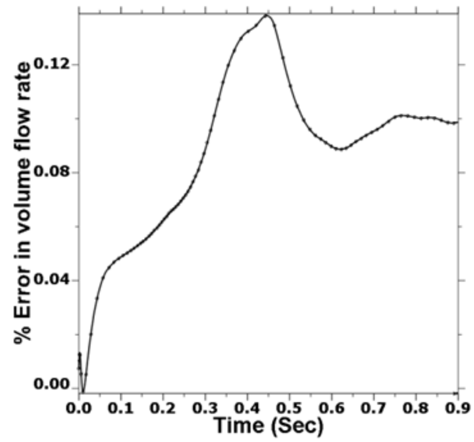

Figures 10 & 11: End systole streamlines (left), mass balance percentage error (right)

Summary

In this technology brief, we demonstrate that Abaqus/CFD can be used to model pulsatile blood flow in the abdominal aorta and the various branches that supply blood to the organs in the abdomen. Newtonian and non-Newtonian blood properties can be modeled and specialized boundary conditions can be implemented with a user subroutine. This study can be easily extended to perform CFD analyses of diseased arteries. Parametric and quantitative studies on various hemodynamic factors could be performed as well. Such studies can offer insight into the temporal and spatial variations of velocity and pressure fields as well as variations of wall shear stresses in vascular geometries.

References

1. C. K. Zarins, D. P. Giddens, B. K. Bharadvaj, V. S. Sottiurai, R. F. Mabon, and S. Glagov, "Carotid bifurcation atherosclerosis: Quantitative correlation of plaque localization with flow velocity profiles and wall shear stress," *Circulation Research*, Vol. 53, pp. 502–514, 1983.
2. J. C. Roberts, C. Moses, and R. H. Wilkins, "Autopsy studies in atherosclerosis: I. Distribution and severity of atherosclerosis in patients dying without morphologic evidence of atherosclerotic catastrophe," *Circulation*, Vol. 20, pp.511–519, 1959.
3. David A. Vorp, "Biomechanics of abdominal aortic aneurysm," *Journal of Biomechanics*, Vol. 40, pp. 1887-1902, 2007.
4. F. Liang, Ryuhei Yamaguchi, H. Liu, "Fluid dynamics in normal and stenosed human renal arteries: an experimental and computational study," *Journal of Biomechanical Science and Engineering*, Vol. 1, pp. 171-182, 2006.
5. D. N. Ku, S. Glagov, J. E. Moore, and C. K. Zarins, "Flow patterns in the abdominal aorta under simulated postprandial and exercise conditions: an experimental study," *Journal of Vascular Surgery*, Vol. 9, pp. 309–316, 1989.
6. Charles A. Taylor, Thomas J.R. Hughes, and Christopher K. Zarins, "Finite Element Modeling of Three-Dimensional Pulsatile Flow in the Abdominal Aorta: Relevance to Atherosclerosis," *Annals of Biomedical Engineering*, Vol. 26, pp. 975-987, 1998.
7. C. J. Mills, I. T. Gabe, J. H. Gault, D. T. Mason, J. Ross Jr., E. Braunwald, and J. P. Shillingford, "Pressure-flow relationships and vascular impedance in man," *Cardiovascular Research*, Vol. 4, pp. 405-417, 1970.
8. C. M. Scotti, E. A. Finol, "Complaint biomechanics of abdominal aortic aneurysms: A fluid-structure interaction study," *Computers and Structures*, Vol. 85, pp. 1097-1113, 2007.
9. J. R. Womersley, "Method for the calculation of velocity, rate of flow and viscous drag in arteries when the pressure gradient is known," *Journal of Physiology*, Vol. 127, pp. 553-563, 1955.
10. J. P. Mynard, P. Nithiarasu, "A 1D arterial blood flow model incorporating ventricular pressure, aortic valve and regional coronary flow using the locally conservative Galerkin (LCG) method," *Communications in Numerical Methods in Engineering*, Vol. 24, pp. 367-417, 2008.
11. Abaqus 6.13 Analysis User's Manual, Dassault Systèmes Simulia Corp, 2013.

About SIMULIA

SIMULIA is the Dassault Systèmes brand that delivers a scalable portfolio of Realistic Simulation solutions including the Abaqus product suite for Unified Finite Element Analysis, multiphysics solutions for insight into challenging engineering problems, and lifecycle management solutions for managing simulation data, processes, and intellectual property. By building on established technology, respected quality, and superior customer service, SIMULIA makes realistic simulation an integral business practice that improves product performance, reduces physical prototypes, and drives innovation. Headquartered in Providence, RI, USA, with R&D centers in Providence and in Velizy, France, SIMULIA provides sales, services, and support through a global network of over 30 regional offices and distributors. For more information, visit www.3ds.com/simulia

Delivering Best-in-Class Products

CATIA
Virtual Product Design

GEOVIA
Virtual Planet

SOLIDWORKS
3D for Professionals

EXALEAD
Information Intelligence

SIMULIA
Realistic Simulation

NETVIBES
Dashboard Intelligence

DELMIA
Virtual Production

3DSWYM
Social Innovation

ENOVIA
Global Collaborative Lifecycle Management

3DVIA
Online 3D Lifelike Experiences

Dassault Systèmes, the **3D**EXPERIENCE Company, provides business and people with virtual universes to imagine sustainable innovations. Its world-leading solutions transform the way products are designed, produced, and supported. Dassault Systèmes' collaborative solutions foster social innovation, expanding possibilities for the virtual world to improve the real world. The group brings value to over 150,000 customers of all sizes in all industries in more than 80 countries. For more information, visit www.3ds.com.

Europe/Middle East/Africa
Dassault Systèmes
10, rue Marcel Dassault
CS 40501
78946 Vélizy-Villacoublay Cedex
France

Asia-Pacific
Dassault Systèmes
Pier City Shibaura Bldg 10F
3-18-1 Kaigan, Minato-Ku
Tokyo 108-002
Japan

Americas
Dassault Systèmes
175 Wyman Street
Waltham, Massachusetts
02451-1223
USA

Visit us at
3DS.COM/SIMULIA